



OPEN

SUBJECT AREAS:

PHYSICAL
OCEANOGRAPHY

ATMOSPHERIC DYNAMICS

Meridional variability of atmospheric convection associated with the Indian Ocean Dipole Mode

Evan Weller & Wenju Cai

Received
30 August 2013Accepted
9 December 2013Published
7 January 2014

Correspondence and
requests for materials
should be addressed to
E.W. (evan.weller@
csiro.au)

CSIRO Water for a Healthy Country Flagship, CSIRO Wealth from Oceans National Research Flagship, CSIRO Marine & Atmospheric Research, Aspendale, VIC, Australia.

The Indian Ocean Dipole Mode (IODM) impacts many surrounding and remote regions of the Indian Ocean, with devastating floods over East Africa but severe droughts in countries surrounding Indonesia during a positive IODM event. Understanding the dynamics is important for seasonal prediction and climate projections, but the role of meridional temperature and circulation anomalies remains unclear. Here, we show that in combination with the zonal structure of temperature and rainfall anomalies, northward contraction of the warm water pool over the eastern equatorial Indian Ocean region (EEIO) also generates an anomalous meridional cross-equatorial temperature gradient in the east. This meridional temperature gradient controls northward retreat of the atmospheric convection in association with northward cross-equatorial winds, and hence declining rainfall over the EEIO. Our results have important implications for the mean state change under greenhouse warming.

Substantial effort has been devoted to understanding the dynamics of the IODM, from its underlying triggers, the associated ocean-atmosphere feedback processes, and to its impacts and predictability, due to the devastating influence on many surrounding and remote regions to the Indian Ocean^{1–11}. During its positive phase, which tends to peak in austral spring, impacts include droughts in Indonesia, East Asia and Australia^{12–17}, flooding to parts of the African continent that lead to malaria^{18–20} and Rift Valley fever virus outbreaks²¹, and even altering regional rainfall over parts of South America²².

The main focus of earlier studies centred on the relationship between the zonal (east-west) sea surface temperature (SST) gradient and zonal wind anomalies over the equatorial Indian Ocean^{1,23–26}, and an east-west shift in the position of atmospheric convection. Little attention has been paid to meridional (north-south) (SST) gradients and related circulation anomalies (especially over the tropical eastern Indian Ocean). This is despite several studies questioning the role of the western Indian Ocean during IODM events^{5,6,27,28}, and raising the issue of whether variability over the western Indian Ocean results simply from perturbations in the eastern Indian Ocean, with anomalies off Sumatra and Java dominating circulation changes during the events.

A subtropical meridional SST gradient in the Southern Hemisphere, sometimes referred to as the Subtropical IOD (SIOD)²⁹, has indeed been shown to have a significant influence on rainfall over East Africa and Australia, and displays a close link with the IODM during austral spring^{30–32}. However this meridional gradient is confined south of the equator and does not involve a cross-equatorial feature. A cross-equatorial meridional SST gradient, closely linked to both El Niño-Southern Oscillation (ENSO) and the IODM, has been shown to peak in boreal spring over the western-central Indian Ocean, important for driving an asymmetric mode of rainfall and wind variability in the tropical central Indian Ocean³³. Such a cross-equatorial meridional SST gradient over the eastern Indian Ocean may similarly play an important role in meridional rainfall and wind variability over the tropics, which could cause large readjustment of the dominant features in the tropical eastern Indian Ocean.

The tropical eastern Indian Ocean comprises the Indian Ocean warm water pool, an area where the southeast trades converge into the South Equatorial Trough associated with the largest convection over the basin, referred to as the oceanic tropical convergence zone (OTCZ), with average rainfall generally greater than 10 mm day^{−1} (ref. 1). As such, the eastern Indian Ocean is rather dynamical: SST variance off Sumatra and Java in austral spring is approximately double that of the western equatorial Indian Ocean; further, cold anomalies in the east are more intense and robust than the warming anomalies in the west, with the centre of warm anomalies varying considerably from one event to another^{34,35}.



In addition, because of the eastern Indian Ocean's close proximity to the Asian continent and the associated strong seasonal Asian monsoon, the mean westerly winds that converge over the EEIO, reduce in June–November. Off Sumatra and Java, when stronger than normal east-to-southeasterly winds prevail, the thermocline is lifted to a depth shallow enough to influence SST, leading to the onset of a positive IODM event^{1–4}. However, in the western Indian Ocean, easterly wind anomalies extend to the far western Indian Ocean and the African coast only during the most extreme IODM years¹⁸, suggesting a response in the west to perturbations in the eastern Indian Ocean.

There is indeed a dipole pattern in convection and rainfall anomalies, which seemingly suggests a westward displacement from the east. Given the relatively muted response in the western Indian Ocean described above, an alternative picture could be that the dipole pattern of convective anomalies results from a westward extension of a weaker convection in the east that also retreats to the north. This would indicate a considerable meridional circulation component over the EEIO associated with the IODM. Here, we explore this possibility by focusing on the meridional SST gradient over the EEIO, assess its relationship with the canonical zonal SST gradient and contraction of the warm water pool and rainfall in the EEIO, and discuss possible implications for the mean state change of the tropical Indian Ocean under climate change. We focus on austral spring (September, October, November, or SON), the season in which an IODM event usually peaks.

Results

Zonal versus meridional SST gradients over the tropical Indian Ocean. Interannual variability in the tropical Pacific (namely ENSO) and Indian (the IODM) oceans involves a perturbation

(strengthening, weakening or reversal) of the zonal walker circulation, primarily in response to the SST anomalies that develop in these tropical regions³⁶. However, indices for monitoring these modes differ: ENSO is monitored by areal mean SST anomalies from several tropical regions spanning the eastern Pacific (Niño 1 + 2: 90°W–80°W, 10°S–0°) to the central-west Pacific (Niño 3.4: 170°W–120°W, 5°S–5°N), whereas the IODM is monitored by a zonal west (IODW: 50°E–70°E, 10°S–10°N) minus east (IOE: 90°E–110°E, 10°S–Equator) anomalous SST gradient over the equatorial Indian Ocean, referred to as the Indian Ocean Dipole Mode Index (DMI)¹ (Fig. 1a). Meridional SST (or heating) gradients can also adjust large scale circulation patterns and lead to changes in the zonal walker circulation^{7,37}. We calculate a meridional SST gradient over the EEIO as the difference in SST anomalies between the northern EEIO (90°E–110°E, 2.5°N–7.5°N) and the southern EEIO (IOE: 90°E–110°E, 10°S–Equator) and compare it to the zonal SST gradient.

As indicated by Fig. 1c, there is almost a unity in the relationship between the zonal and meridional SST gradients over the tropical Indian Ocean during austral spring. A highly significant correlation of 0.96 emphasises this. Also evident in the scatter diagram is that both gradients are positively skewed: there is a tendency for the amplitude of both SST gradients to be larger during positive IODM events, compared to negative events, a feature well documented for the zonal SST gradient^{11,38}. We believe this is the first time that it has been shown that the meridional SST gradient also possesses the same skewness. A positive IODM event is commonly defined as when the zonal anomalous SST gradient, referenced to a mean climate³⁹ (here we reference to the study period), exceeds a threshold value of its variance. Using a one-standard deviation value as a threshold for demonstration (gray dashed box in Fig. 1c), the IODM in 1982, 1994, 1997, and 2006 are noted as strong positive

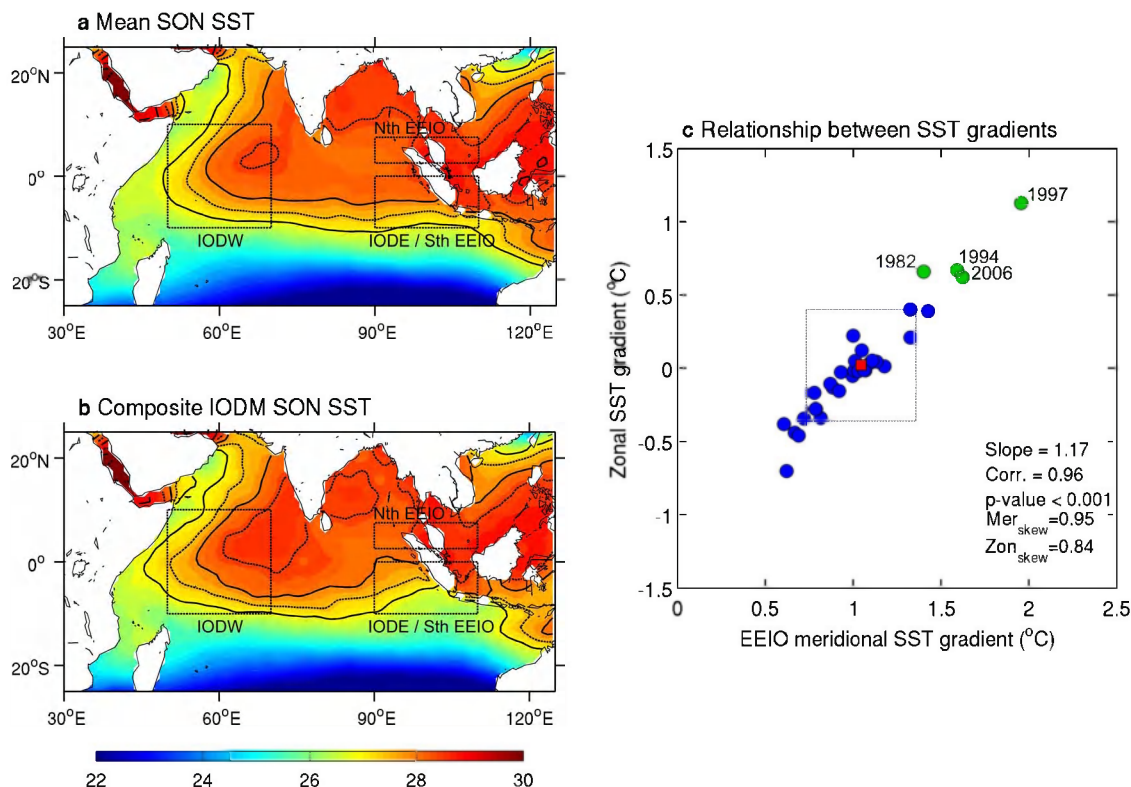


Figure 1 | Indian Ocean austral spring (SON) SSTs. Composites of the SON (a), mean SST and (b), SST during positive Indian Ocean Dipole Mode (IODM) events as indicated in (c). The solid and dashed contours denote isotherms greater than 27°C at 0.5°C increments. (c), SON mean zonal SST gradient (Dipole Mode Index (DMI)) versus the eastern equatorial Indian Ocean (EEIO) meridional SST gradient during 1979–2010. In (c) the red square denotes the mean, and the surrounding box the ± 1 standard deviation departure from the mean. Years defined as positive IODM events are shown in green with the year indicated. All maps and plots were produced using licensed MATLAB.



IODM events (green markers in Fig. 1c), during 1979 to 2010, in line with other previous work^{7,8,40}. As expected with the high correlation shown in Fig. 1c, following the same criteria, using the meridional SST gradient identifies the same years when a strong positive IODM occurred. Although other positive IODM events have occurred over this time period^{18,14,40}, our classification does not emphasise these weaker events as they only displayed moderate amplitudes and SST gradients. A large meridional SST gradient (greater than 1 standard deviation) occurred during 1987; however it was concurrent with only a moderate zonal SST gradient, therefore is also excluded.

When compared to the mean climatology (Fig. 1a), a composite map of austral spring SST during strong IODM events reveals several noteworthy features in addition to those commonly identified with positive IODM events (Fig. 1b). In the central-western equatorial Indian Ocean, SST increases which supports an increase in convection (Fig. 2a). Yet, the SST adjacent to the African continent does not appear to increase much in the composite. In addition, there is some mild cooling in the Bay of Bengal, but in the EEIO, SST north of the equator remains relatively unchanged. However, with the dramatic cooling south of the equator off Sumatra and Java, the isotherms over the EEIO can be seen to contract northward towards the equator (Fig. 1b), thus increasing the EEIO meridional SST gradient. As the EEIO is generally the region of highest rainfall (Fig. 2b) and we have shown that the EEIO meridional SST gradient is highly correlated with the zonal SST gradient, we examine the northward contraction of the warm waters towards the equator further in order to unveil the importance of meridional anomalies in the EEIO dynamics during IODM events (Fig. 1b), and its relationship with rainfall in this region.

Interannual variability of warm water pool contraction over the EEIO. To test the interannual variability of the northward contraction of the warm water pool over the EEIO, we select the 27°C isotherm, because on average, it is situated on the southern boundary of the IODE at ~10°S (Fig. 1a), and track its mean position during each austral spring between 90°E–110°E. Similar results are obtained if we select other values such as the 28°C isotherm. Over the IODE region, rainfall is negatively skewed and generally high during austral spring (mean rainfall of ~8 mm day⁻¹), with occurrences of episodic large reductions occurring since 1979, but without occurrences of comparably large episodic increases (x-axis, Fig. 3a). As evident by the average latitude of the 27°C isotherm, when the south EEIO region cools, the isotherm retreats towards the equator in a close relationship with a reduction in the local rainfall (Fig. 2c and 3a). Rainfall decreases by more than 50% during years that display maximum northward contraction of the warm water pool. On the other hand, the two wettest years do not correspond to the southernmost latitude of the 27°C isotherm, reflecting a tighter relationship between the two variables when the warm water is retreating northward than when the warm water is expanding southward. The dynamics is similar to that associated with south EEIO negative SST skewness: the retreat occurs when the thermocline is shallowing, therefore exerting a greater cooling impact on SST than the warming effect when the thermocline is deepening^{11,41,42}; the greater cooling in turn causes a greater damping with a greater rainfall response¹⁴.

The northward contraction of the warm water pool over the EEIO displays the same level of correlation with both zonal (Fig. 3b) and meridional (Fig. 3c) SST gradients over the equatorial Indian Ocean. These scatter diagrams highlight that maximum contraction of the warm water pool indeed occurs when both gradients are strongly positive, i.e. during positive IODM events. This provides support that the meridional SST gradient could be as dominant as the zonal SST gradient in driving the circulation anomalies that lead to large rainfall anomalies during austral spring, such as the reduction over the EEIO.

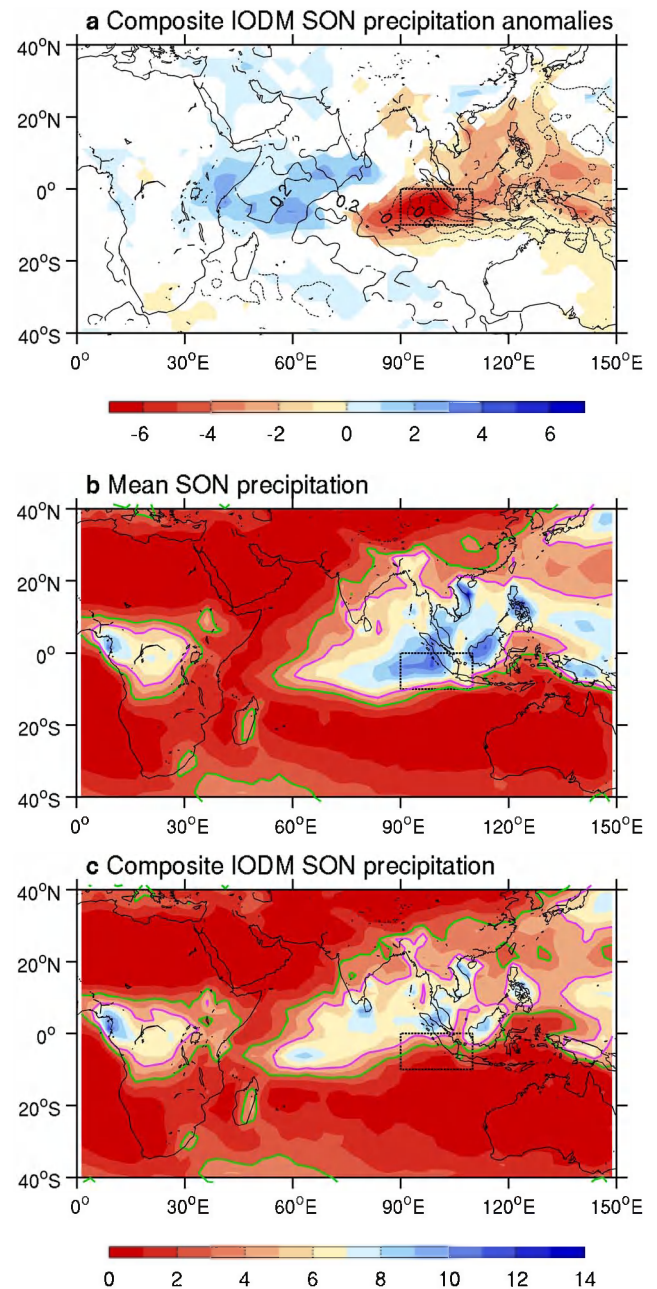


Figure 2 | Indian Ocean austral spring (SON) mean rainfall and anomalies during positive IODM events. (a), Composite of SON rainfall (shading) anomalies during positive IODM events. Contours also indicate the associated SST anomalies. Only anomalies exceeding 90% significance (estimated by the two-tailed t-test) are shown. Composites of the SON (b), mean rainfall and (c), rainfall during positive IODM events. In (b) and (c), the 3 and 5 mm day⁻¹ contours are indicated by the green and magenta contours, respectively, to highlight the position of the OTCZ high rainfall band. All plots were produced using licensed MATLAB.

Interestingly, over the central-western Indian Ocean, the SST in the IODW region only has a faintly higher correlation with the zonal SST gradient than with the EEIO meridional SST gradient, with correlations of 0.71 and 0.66, respectively (figure not shown). Therefore it is plausible that EEIO meridional SST gradients are an integral forcing of large scale circulations over the equatorial Indian Ocean, and that SST anomalies in the central-west Indian Ocean are simply a response to such circulation anomalies^{5,27,28}.

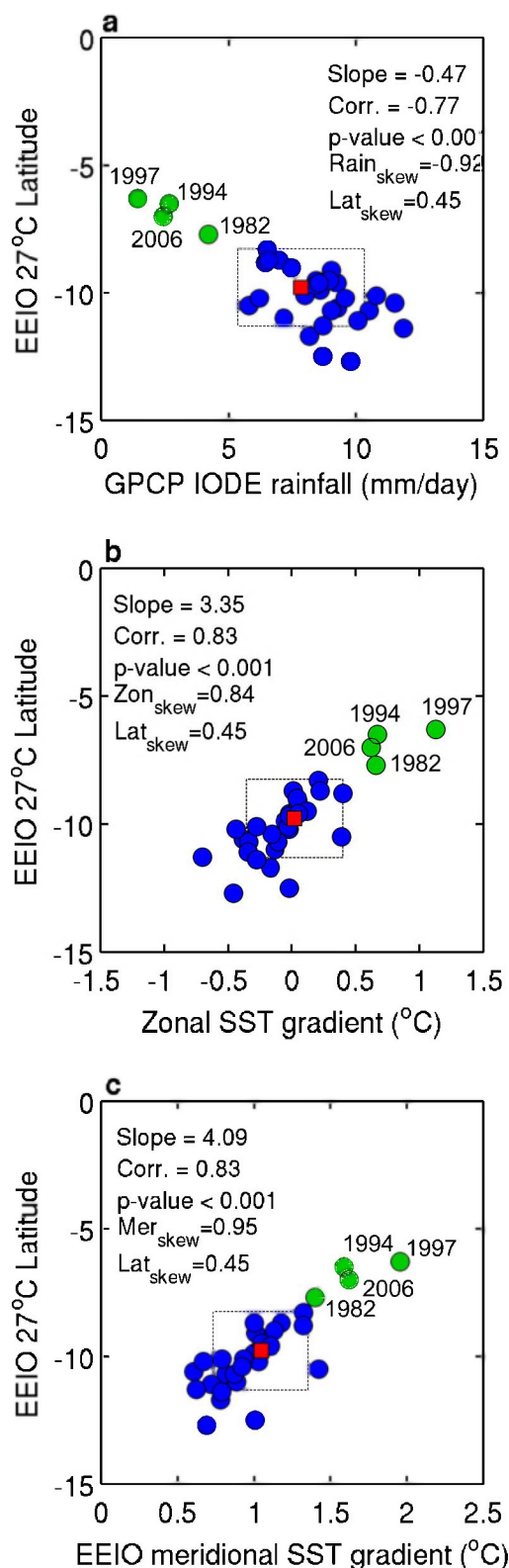


Figure 3 | Relationship of warm water contraction with rainfall and SST gradients. (a), Austral spring (SON) mean latitude (between 90°E–110°E) of the 27°C isotherm in the EEIO versus the IODE rainfall during 1979–2010. (b), As in (a) but for the EEIO 27°C isotherm versus the zonal SST gradient (DMI). (c), As in (a) but for the EEIO 27°C isotherm versus the EEIO meridional SST gradient. The red square denotes the mean, and the surrounding box the ± 1 standard deviation departure from the mean. Years defined as positive IODM events are shown in green with the year indicated. All plots were produced using licensed MATLAB.

Relationship of rainfall reduction with SST gradients. The linkage between the zonal SST gradient during positive IODM events and devastating droughts for many neighbouring regions of the EEIO was identified^{12–17}. Fig. 4a highlights that in the post-satellite data since 1979 presented here, the most extreme IODM event in austral spring 1997, reduced rainfall to $\sim 20\%$ of the seasonal mean over the IODE region. Over the EEIO, where the southeast trades converge into the OTCZ, the meridional SST gradient explains the same level of variance in the interannual variability of the rainfall as the zonal SST gradient (when comparing the correlation coefficients in Fig. 4a and b). The scatter diagrams indicate that, in addition to a strongly negative correlation of -0.86 , when both the zonal or meridional SST gradients are largely positive, (i.e. positive IODM events), the rainfall over the IODE is dramatically reduced. Again, there is far weaker association between the SST gradients and rainfall during wetter than average years, but the relationship during positive IODM events is robust.

Expanding the examination of the relationship for the IODE region shown in Figure 4 during IODM events, we see that such large reductions in rainfall in the OTCZ south of the equator can facilitate the development of a large scale north-south heating (precipitation) gradient. Together with the meridional SST gradient, this can enforce meridional circulation anomalies (Fig. 5a) such as the strong anomalous winds off the Sumatra and Java coasts that extend over the equator^{6,7,37}. The circulation anomalies can potentially transport moisture away from the region and further north into the monsoon trough⁷, or west of the normal position of the OTCZ where the perturbed southeast trade winds converge further downstream and moisture is supplied at the extended end of the trade winds¹. We can utilise observed global rainfall data to investigate the anomalous rainfall patterns during IODM events over the entire Indian Ocean and impacted surrounding regions.

Shifts in the rainfall pattern associated with the IODM. There is debate on the dynamics relating to the anomalous rainfall during IODM events and whether or not increased rainfall over the western Indian Ocean and flooding to East Africa is simply due to a shift of the rainfall from the EEIO where droughts ensue^{1,2,18,23,24,30}. Here we construct both anomalous (composite mean minus climatological mean) and absolute rainfall patterns during austral spring when both the zonal or meridional SST gradients are largely positive, during the identified IODM events of 1982, 1994, 1997, and 2006. We note that these events also coincide with developing El Niño, raising the question as to whether the responses are due to external forcing rather than an independent mode of Indian Ocean variability^{5,24,43}. We do not attempt to address this here, instead we concentrate on the overall circulation anomalies and rainfall patterns associated with the SST gradients over the equatorial Indian Ocean as detailed in the earlier sections.

The dashed box in Fig. 2a over the EEIO highlights the IODE region where convection reduces when the zonal or meridional SST gradients are largely positive (Fig. 4b and c). It is evident that this is a region where the largest reductions in rainfall over the EEIO occurs (red shading in Fig. 2a). Significant negative anomalies are evident further west over the OTCZ south of the equator to $\sim 75^\circ\text{E}$, and east of 90°E , negative anomalies can be seen over the maritime continent and the western Pacific. The composite highlights that during the IODM events identified here, apart from the southern Indian subcontinent and Sri Lanka where there are considerable rainfall increases^{44,45}, there appears to be very little influence further north over the northern Indian subcontinent and the Asian continent in the post-monsoon season, unlike the positive relationship during the peak monsoon season during boreal summer^{7,46}. This is supported by the fact that there is minimal transport of moisture to the north during these years in austral spring (Fig. 5b). Therefore, when the meridional SST gradient increases in this season,

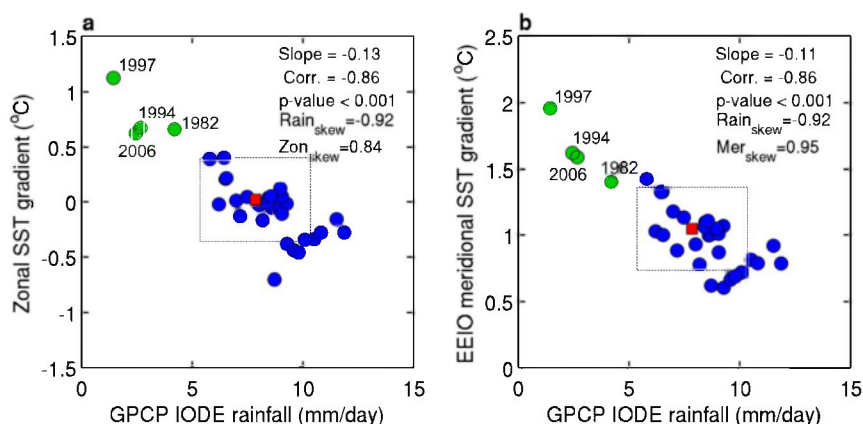


Figure 4 | Relationship of rainfall with SST gradients. (a), Austral spring (SON) mean IODE rainfall versus the zonal SST gradient (DMI) during 1979–2010. (b), As is (a) but for the IODE rainfall versus the EEIO meridional SST gradient. The red square denotes the mean, and the surrounding box the ± 1 standard deviation departure from the mean. All plots were produced using licensed MATLAB.

convection weakens and occurs only over the northern EEIO in response to the warm water contraction to the equator (Fig. 2c). The weakened convection is consistent with the feature that SSTs are little changed, if not slightly decreased north of the equator (Fig. 1b).

The dipole pattern of rainfall anomalies across the equatorial Indian Ocean (Fig. 2a) that has previously been noted during IODM events gives an impression that a shift in the locus of atmospheric convection from the east to the west has occurred to bring floods to East Africa. However this is not the case when a composite of the absolute rainfall (Fig. 2c) is compared with the climatological mean rainfall (Fig. 2b). These maps highlight that the positive rainfall anomalies in Fig. 2a turn out to be a result from two sources. Firstly, a westward extension of the OTCZ over the central-western equatorial Indian Ocean is evident (comparing Fig. 2c to Fig. 2b). By indicating the 3 and 5 mm day⁻¹ contours in Fig. 2b and c, the westward expansion of the rainfall band associated with the OTCZ, becomes clear. When the zonal and meridional SST gradients are strongly positive, stronger than normal southeasterly winds over the southern Indian Ocean cause the trade winds to extend, which converge further downstream (Fig. 5a). This enhances the convergence and moisture supply (Fig. 5b) at the extended downstream end of the trade winds in the OTCZ¹. However, these contours also highlight the fact positive rainfall anomalies over equatorial Africa do not result from the extension of the OTCZ, consistent with other studies^{18,30}.

Discussion

This study highlights that there is a meridional SST gradient in the EEIO of the same magnitude as the basin wide zonal SST gradient during austral spring associated with the IODM. While this supports the notion that the EEIO is the main region of activity during IODM events, coinciding with the warmest waters and largest convection over the basin, a new finding of this study is that there is just as close a relationship between the rainfall over the south EEIO (IODE region) and the meridional SST gradient as with the zonal SST gradient during the post-satellite era investigated events. This highlights the importance of meridional circulation anomalies. Both SST gradients are associated with a northward contraction of the warm water pool over the EEIO. By representing this contraction simply by following the latitude of the 27°C isotherm over the EEIO, we reveal a good relationship between the strength of both SST gradients and the extent to which the warm waters contract. The strength of reduction in rainfall over the equatorial southeast Indian Ocean is also related to the contraction of the warm water pool to the north during positive IODM events. The IODE rainfall has previously been shown to be closely related to the zonal SST gradient during IODM events;

however the findings we show here is that the IODE rainfall is as closely related to the meridional SST gradient over the EEIO, with the same level of correlation.

We also show that unlike the positive relationship of the IODM and increased Indian subcontinent and Asian continent rainfall in the peak monsoon season in boreal summer, there appears very little

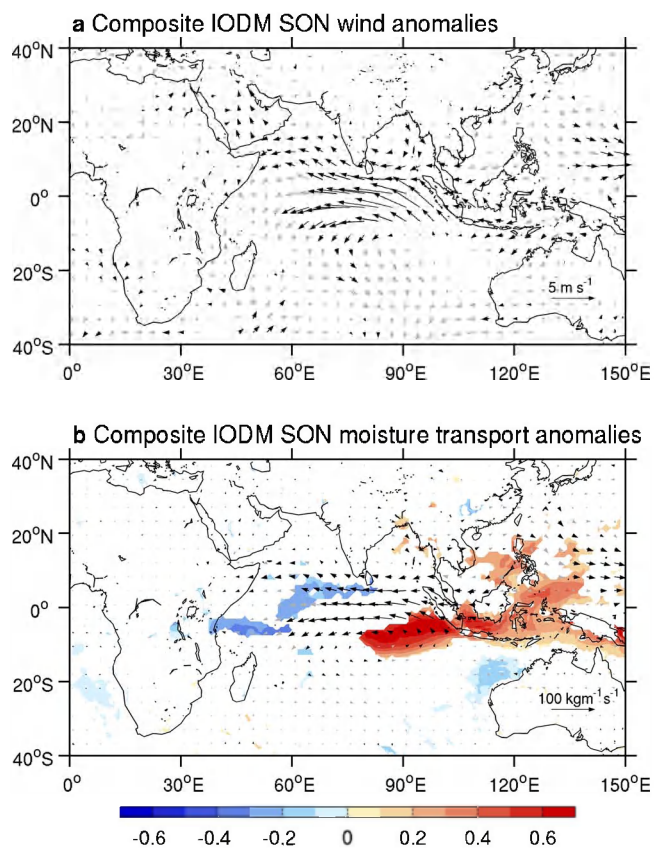


Figure 5 | Indian Ocean austral spring (SON) wind and moisture transport anomalies during positive IODM events. (a), Composite of SON surface wind anomalies during positive IODM events. (b), Composite of SON divergence (shading) and vertically integrated water vapour flux (arrows) anomalies during positive IODM events. The black arrows in (a) and (b), and shading in (b), indicate anomalies exceeding 90% significance (estimated by the two-tailed t-test). All plots were produced using licensed MATLAB.



transport of moisture from the EEIO or western Indian Ocean further north in the post-monsoon season, with rainfall reductions seen over the entire eastern part of the Indian Ocean basin, east of $\sim 90^\circ\text{E}$. The comparison of anomalous and absolute rainfall patterns during strong IODM events with the climatological mean highlights that although there is minimal transport of moisture to the north over the EEIO, there is some extension of the OTCZ westward with increased easterly anomalies and redirection of the flow.

Under greenhouse warming, the EEIO meridional SST gradient could be an important component of the future mean state for the EEIO region. In the Indian Ocean, SST is projected to warm faster in the west than off the Sumatra and Java coasts in the east, thus increasing the zonal SST gradient and facilitating in a reduced strength of the equatorial westerly winds during austral spring^{42,47–49}. However, in the eastern Indian Ocean, the north is also projected to warm faster than the south, due to its close proximity to the Asian landmass, translating to an increase in the mean meridional SST gradient that somewhat resembles the condition during the positive phase of the present-day IODM. This can potentially be a mechanism whereby changes in the mean meridional SST gradient, contributed by the remote faster warming land mass to the north, influences mean zonal SST gradients and winds of the equatorial Indian Ocean toward the projected mean state change in the equatorial Indian Ocean.

Methods

Data. The analysis utilises Met Office Hadley Centre's SST data set (HadISST) v1.1⁵⁰ to monitor tropical SST variability. The Indian Ocean Dipole Mode is described through an anomalous zonal SST gradient over the equatorial Indian Ocean, referred to as the Indian Ocean Dipole Mode Index (DMI)¹, defined as the difference of the area mean SST anomalies in the western Indian Ocean (IODW) region (10°S – 10°N , 50° – 70°E) and the eastern Indian Ocean (IODE) region (10°S –Equator, 90° – 110°E). We calculate a meridional SST gradient over the eastern equatorial Indian Ocean (EEIO) as the difference in SST anomalies between the northern EEIO (90°E – 110°E , 2.5°N – 7.5°N) and the southern EEIO (IODE: 90°E – 110°E , 10°S –Equator). The results are robust to the exclusion of SSTs east of the Indonesian and Malaysian landmasses in the boxes over which the SSTs are calculated in the eastern Indian Ocean (Fig. 1a). Precipitation data from version 2 of the Global Precipitation Climatology Project (GPCP) analysis⁵¹, and wind stress, divergence and vertically integrated water vapour flux from the ERA-Interim reanalysis⁵², spanning from 1979–2010, is used to diagnose mean seasonal circulation and convection patterns.

Seasonality. All calculations in this paper are based on data in austral spring (September, October, and November, or SON). In this season, the observed Indian Ocean Dipole Mode is at its peak phase.

Graphic software. All maps and plots were produced using licensed MATLAB.

1. Saji, N. H., Goswami, B. N., Vinayachandran, P. N. & Yamagata, T. A dipole mode in the tropical Indian Ocean. *Nature* **401**, 360–363 (1999).
2. Webster, P. J., Moore, A. M., Loschnigg, J. P. & Leben, R. R. Coupled oceanic-atmospheric dynamics in the Indian Ocean during 1997–98. *Nature* **401**, 356–360 (1999).
3. Yu, L. & Rienecker, M. M. Mechanisms for the Indian Ocean warming during the 1997–98 El Niño. *Geophys. Res. Lett.* **26**, 735–738 (1999).
4. Murtugudde, R., McCreary, J. P. & Busalacchi, A. J. Oceanic processes associated with anomalous events in the Indian Ocean with relevance to 1997–1998. *J. Geophys. Res.* **105**, 3295–3306 (2000).
5. Allan, R. J. *et al.* Is there an Indian Ocean dipole, and is it independent of the El Niño–Southern Oscillations? *CLIVAR Exchanges* **6**, 18–22 (2001).
6. Hastenrath, S. Dipoles, temperature gradients and tropical climate anomalies. *BAMS* **83**, 735–738 (2002).
7. Annamalai, H., Murtugudde, R., Wang, B., Potemra, J. & Xie, S.-P. Coupled dynamics in the Indian Ocean: Spring initiation of the Zonal Mode. *Deep-Sea Res. II* **50**, 2305–2330 (2003).
8. Saji, N. H. & Yamagata, T. Possible impacts of Indian Ocean Dipole mode events on global climate. *Climate Res.* **25**, 151–169 (2003).
9. Zheng, X. T., Xie, S.-P., Vecchi, G. A., Liu, Q. & Hafner, J. Indian Ocean dipole response to global warming: Analysis of ocean-atmospheric feedbacks in a coupled model. *J. Clim.* **23**, 1240–1253 (2010).
10. Liu, L., Yu, W. & Li, T. Dynamic and thermodynamic air-sea coupling associated with the Indian Ocean Dipole diagnosed from 23 WCRP CMIP3 models. *J. Clim.* **24**, 4941–4958 (2011).
11. Ogata, T., Xie, S.-P., Lan, J. & Zheng, X. Importance of ocean dynamics for the skewness of the Indian Ocean Dipole mode. *J. Clim.* **26**, 2145–2159 (2013).

12. Abram, N. J., Gagan, M. K., McCulloch, M. T., Chappell, J. & Hantoro, W. S. Coral reef death during the 1997 Indian Ocean Dipole linked to Indonesian wildfires. *Science* **301**, 952–955 (2003).
13. Ashok, K., Guan, Z. & Yamagata, T. Influence of the Indian Ocean Dipole on the Australian winter rainfall. *Geophys. Res. Lett.* **30**, L1821 (2003).
14. Cai, W., Cowan, T. & Sullivan, A. Recent unprecedented skewness towards positive Indian Ocean Dipole occurrences and its impact on Australian rainfall. *Geophys. Res. Lett.* **36**, L11705 (2009).
15. Ummenhofer, C. C. *et al.* What causes southeast Australia's worst droughts? *Geophys. Res. Lett.* **36**, L04706 (2009).
16. Kripalani, R. H., Oh, J. H. & Chaudhari, H. S. Delayed influence of the Indian Ocean Dipole mode on the East Asia–West Pacific monsoon: possible mechanism. *Int. J. Climatol.* **30**, 197–209 (2010).
17. Cai, W., van Rensch, P., Cowan, T. & Hendon, H. H. An asymmetry in the IOD and ENSO teleconnection pathway and its impact on Australian climate. *J. Clim.* **25**, 6318–6329 (2012).
18. Black, E., Slingo, J. & Sperber, K. R. An observational study of the relationship between excessively strong short rains in coastal East Africa and Indian Ocean SST. *Mon. Wea. Rev.* **131**, 74–94 (2003).
19. Behera, S. K. *et al.* Paramount impact of the Indian Ocean Dipole on the East African short rains: A CGCM study. *J. Clim.* **18**, 4514–4530 (2005).
20. Hashizume, M., Chaves, L. F. & Minakawa, N. Indian Ocean Dipole drives malaria resurgence in East African highlands. *Sci. Rep.* **2**, 269 (2012).
21. Linthicum, K. J. *et al.* Climate and satellite indicators to forecast Rift Valley fever epidemics in Kenya. *Science* **285**, 397–400.
22. Chan, S. C., Behera, S. K. & Yamagata, T. Indian Ocean Dipole influence on South American rainfall. *Geophys. Res. Lett.* **35**, L14S12 (2008).
23. Reverdin, G., Cadel, D. & Gutzler, D. Interannual displacements of convection and surface circulation over the equatorial Indian Ocean. *Q. J. R. Meteorol. Soc.* **112**, 43–67 (1986).
24. Hastenrath, S., Nicklis, A. & Greischar, L. Atmospheric-hydrospheric mechanisms of climate anomalies in the western equatorial Indian Ocean. *J. Geophys. Res.* **98**, 20219–20235 (1993).
25. Udea, H. & Matsumoto, J. A. Possible triggering process of east–west asymmetric anomalies over the Indian Ocean in relation to 1997/1998 El Niño. *J. Meteor. Soc. Japan* **78**, 803–818 (2000).
26. Xie, S.-P., Annamalai, H., Schott, F. & McCreary Jr, J. P. Origin and predictability of South Indian Ocean climate variability. *J. Clim.* **15**, 864–874 (2002).
27. Dommenget, D. & Latif, M. A. Cautionary Note on the Interpretation of EOFs. *J. Clim.* **15**, 216–225 (2002).
28. Baquero-Bernal, A., Latif, M. & Legutke, S. On dipole-like variability in the tropical Indian Ocean. *J. Clim.* **15**, 1358–1368 (2002).
29. Behera, S. K. & Yamagata, T. Subtropical SST dipole events in the southern Indian Ocean. *Geophys. Res. Lett.* **28**, 327–330 (2001).
30. Ummenhofer, C. C., Gupta, A. S., England, M. H. & Reason, C. J. Contributions of Indian Ocean sea surface temperatures to enhanced East African rainfall. *J. Clim.* **22**, 993–1013 (2009a).
31. Ummenhofer, C. C., Gupta, A. S., Taschetto, A. S. & England, M. H. Modulation of Australian precipitation by meridional gradients in east Indian Ocean sea surface temperatures. *J. Clim.* **22**, 5597–5610 (2009b).
32. Ummenhofer, C. C. *et al.* Pacific Ocean contribution to the asymmetry in eastern Indian Ocean variability. *J. Clim.* **26**, 1152–1171 (2013).
33. Wu, R., Kirtman, B. P. & Krishnamurty, V. An asymmetric mode of tropical Indian Ocean rainfall variability in boreal spring. *J. Geophys. Res.* **113**, D05104 (2008).
34. Le Blanc, J. L. & Boulanger, J. P. Propagation and reflection of long equatorial waves in the Indian Ocean from TOPEX/POSEIDON data during the 1993–1998 period. *Clim. Dyn.* **17**, 547–557 (2001).
35. Huang, B. & Kinter, J. L. The interannual variability in the tropical Indian Ocean and its relations to El Niño–Southern Oscillation. *J. Geophys. Res.* **107**, 3199 (2002).
36. Rao, A. S., Behera, S. K., Masumoto, Y. & Yamagata, T. Interannual variability in the subsurface tropical Indian Ocean. *Deep-Sea Res. II* **49**, 1549–1572 (2002).
37. Gill, A. E. Some simple solutions for heat induced tropical circulation. *Quart. J. R. Met. Soc.* **106**, 447–462 (1980).
38. Hong, C. C., Li, T., Lin, H. & Kug, J. S. Asymmetry of the Indian Ocean Dipole. Part I: Observational Analysis. *J. Clim.* **21**, 4834–4848 (2008).
39. Alley, R. *et al.* [Summary for policymakers] *Climate change 2007: The physical science basis* [Solomon, S. *et al.* (ed.)] (Cambridge University Press, Cambridge, 2007).
40. Meyers, G. A., McIntosh, P. C., Pigot, L. & Pook, M. J. The years of El Niño, La Niña, and interactions with the tropical Indian Ocean. *J. Clim.* **20**, 2872–2880 (2007).
41. Cai, W. & Qiu, Y. An observation-based assessment of nonlinear feedback processes associated with the Indian Ocean Dipole. *J. Clim.* **26**, 2880–2890 (2013).
42. Zheng, X. T. *et al.* Indian Ocean Dipole response to global warming in the CMIP5 multi-model ensemble. *J. Clim.* **26**, 6067–6080 (2013).
43. Luo, J. J. *et al.* Interaction between El Niño and Extreme Indian Ocean Dipole. *J. Clim.* **23**, 726–742 (2010).
44. Zubair, L., Rao, S. A. & Yamagata, T. Modulation of Sri Lankan Maha rainfall by the Indian Ocean dipole. *Geophys. Res. Lett.* **30**, 1063 (2003).



45. Kripalani, R. H. & Kumar, P. Northeast monsoon rainfall variability over South Peninsula India vis-à-vis the Indian Ocean Dipole Mode. *Inter. J. Clim.* **24**, 1267–1282 (2004).
46. Ashok, K. & Saji, N. H. On the impacts of ENSO and Indian Ocean dipole events on sub-regional Indian summer monsoon rainfall. *Nat. Hazards* **42**, 273–285 (2007).
47. Vecchi, G. A. & Soden, B. J. Global warming and the weakening of the tropical circulation. *J. Clim.* **20**, 4316–4340 (2007).
48. Xie, S.-P. *et al.* Global warming pattern formation: sea surface temperature and rainfall. *J. Clim.* **23**, 966–986 (2010).
49. Huang, P., Xie, S.-P., Hu, K., Huang, G. & Huang, R. Patterns of the seasonal response of tropical rainfall to global warming. *Nature Geosci* **6**, 357–361 (2013).
50. Rayner, N. A. *et al.* Global analyses of sea surface temperature, sea ice, and night marine air temperature since the late nineteenth century. *J. Geophys. Res.* **108**, 4407 (2003).
51. Adler, R. F. *et al.* The Version 2 Global Precipitation Climatology Project (GPCP) Monthly Precipitation Analysis (1979–Present). *J. Hydrometeor.* **4**, 1147–1167 (2003).
52. Dee, D. P. *et al.* The ERA-Interim reanalysis: configuration and performance of the data assimilation system. *Q. J. R. Meteorol. Soc.* **137**, 553–597 (2011).

Acknowledgments

This research is partly supported by the CSIRO Water for a Healthy Country Flagship, the CSIRO Wealth from Oceans National Research Flagship, The Goyder Institute for Water Research, and the Australian Climate Change Science Programme.

Author contributions

E.W. and W.C. contributed to designing the research and interpreting the results. E.W. analysed the observation data and wrote the manuscript.

Additional information

Competing financial interests: The authors declare no competing financial interests.

How to cite this article: Weller, E. & Cai, W. Meridional variability of atmospheric convection associated with the Indian Ocean Dipole Mode. *Sci. Rep.* **4**, 3590; DOI:10.1038/srep03590 (2014).



This work is licensed under a Creative Commons Attribution-NonCommercial-NoDerivs 3.0 Unported license. To view a copy of this license, visit <http://creativecommons.org/licenses/by-nc-nd/3.0>